

PAPER • OPEN ACCESS

## Exploring the partonic phase at finite chemical potential within a covariant off-shell transport approach

To cite this article: E Soloveva *et al* 2020 *J. Phys.: Conf. Ser.* **1667** 012040

View the [article online](#) for updates and enhancements.

### You may also like

- [Dilepton production at SPS and RHIC energies within the PHSD off-shell transport approach](#)  
O Linnyk, E L Bratkovskaya and W Cassing
- [Non-Hermitian topological phases and dynamical quantum phase transitions: a generic connection](#)  
Longwen Zhou and Qianqian Du
- [Dynamical quantum phase transitions: a review](#)  
Markus Heyl



## Breath Biopsy® OMNI®

The most advanced, complete solution for global breath biomarker analysis

TRANSFORM YOUR RESEARCH WORKFLOW



Expert Study Design & Management



Robust Breath Collection



Reliable Sample Processing & Analysis



In-depth Data Analysis



Specialist Data Interpretation

# Exploring the partonic phase at finite chemical potential within a covariant off-shell transport approach

O E Soloveva<sup>1</sup>, P Moreau<sup>1</sup>, L Oliva<sup>1</sup>, T Song<sup>1,2</sup>,  
E L Bratkovskaya<sup>1,2</sup>, W Cassing<sup>3</sup>

<sup>1</sup> Institut für Theoretische Physik, Goethe-Universität Frankfurt am Main, Germany

<sup>2</sup> GSI Helmholtzzentrum für Schwerionenforschung GmbH, Darmstadt, Germany

<sup>3</sup> Institut für Theoretische Physik, Justus-Liebig-Universität Giessen, Germany

E-mail: soloveva@fias.uni-frankfurt.de

**Abstract.** We report on the extended Parton-Hadron-String Dynamics (PHSD) transport approach in the partonic sector by explicitly calculating the total and differential partonic scattering cross sections as a function of temperature  $T$  and baryon chemical potential  $\mu_B$  on the basis of the effective propagators and couplings from the Dynamical QuasiParticle Model (DQPM). We calculated the ratio of shear viscosity  $\eta$  over entropy density  $s$ , i.e.  $\eta/s$  is evaluated using the collisional widths and compared to lQCD calculations for  $\mu_B = 0$  as well. We find that the ratio  $\eta/s$  does not differ very much from that calculated within the original DQPM on the basis of the Kubo formalism. Furthermore, there is only a very modest change of  $\eta/s$  with the baryon chemical  $\mu_B$  as a function of the scaled temperature  $T/T_c(\mu_B)$ . This also holds for a variety of hadronic observables from central A+A collisions in the energy range  $5 \text{ GeV} \leq \sqrt{s_{NN}} \leq 200 \text{ GeV}$  when implementing the differential cross sections into the PHSD approach. Accordingly, it will be difficult to extract finite  $\mu_B$ -signals from the partonic dynamics based on bulk observables.

## 1. Introduction

The phase transition from hadronic matter to a quark-gluon plasma (QGP) is a central topic of modern high-energy physics. A study of the properties of the hot and dense quark-gluon plasma is fascinating from both theoretical and experimental points of view. In order to investigate the dynamics and relevant scales of this phase transition laboratory experiments under controlled conditions are performed with relativistic nucleus-nucleus collisions. In order to explore these collisions one can use the parton-hadron-string dynamics (PHSD) transport approach [1] which reliably describes observables from p+A and A+A collisions from SPS to LHC energies including electromagnetic probes such as photons and dileptons [2].

The new facilities FAIR and NICA, which are under construction, will probe the region of the QCD phase diagram at higher net baryon density and  $\mu_B$ , respectively. In order to explore the partonic systems at higher  $\mu_B$ , the PHSD approach is extended to incorporate partonic quasiparticles and their differential cross sections that depend on  $T$  and  $\mu_B$  explicitly.



## 2. PHSD

The parton-hadron-string dynamics (PHSD) approach is an off-shell transport approach based on Kadanoff-Baym equations in first-order gradient expansion [3] employing resummed propagators from the dynamical quasiparticle model (DQPM). We have calculated the partonic differential cross sections as a function of  $T$  and  $\mu_B$  for the leading tree-level diagrams using the DQPM (cf. Appendices of Ref. [4]). In order to explore the transport properties of a partonic system we have calculated the interaction rates using these differential cross sections as a function of temperature and baryon chemical potential (cf. Ref. [4]). In the on-shell case (energies of the particles are taken to be  $E^2 = \mathbf{p}^2 + M^2$  with  $M$  being the pole mass) the interaction rate  $\Gamma^{on}$  is obtained as follows:

$$\begin{aligned} \Gamma_i^{on}(p_i, T, \mu_q) &= \frac{1}{2E_i} \sum_{j=q,\bar{q},g} \int \frac{d^3p_j}{(2\pi)^3 2E_j} d_j f_j(E_j, T, \mu_q) \int \frac{d^3p_3}{(2\pi)^3 2E_3} \\ &\times \int \frac{d^3p_4}{(2\pi)^3 2E_4} (1 \pm f_3)(1 \pm f_4) |\bar{\mathcal{M}}|^2(p_i, p_j, p_3, p_4) (2\pi)^4 \delta^{(4)}(p_i + p_j - p_3 - p_4) \\ &= \sum_{j=q,\bar{q},g} \int \frac{d^3p_j}{(2\pi)^3} d_j f_j v_{rel} \int d\sigma_{ij \rightarrow 34}^{on} (1 \pm f_3)(1 \pm f_4), \end{aligned} \quad (1)$$

where  $d_j$  is the degeneracy factor for spin and color (for quarks  $d_q = 2 \times N_c$  and for gluons  $d_g = 2 \times (N_c^2 - 1)$ ), and with the shorthand notation  $f_j = f_j(E_j, T, \mu_q)$  for the distribution functions. In Eq. (1) and in all the following sections, the notation  $\sum_{j=q,\bar{q},g}$  includes the contribution from all possible partons which in our case are the gluons and the (anti-)quarks of three different flavors ( $u, d, s$ ).

## 3. Transport properties of the partonic system

The starting point to evaluate viscosity coefficients of partonic matter is the Kubo formalism [5] which was also used to calculate the viscosities within the PHSD in a box with periodic boundary conditions (cf. Ref. [6]). We focus here on the calculation of the shear viscosity based on Ref. [7] which reads:

$$\eta^{\text{Kubo}}(T, \mu_q) = - \int \frac{d^4p}{(2\pi)^4} p_x^2 p_y^2 \sum_{i=q,\bar{q},g} d_i \frac{\partial f_i(\omega)}{\partial \omega} \rho_i(\omega, \mathbf{p})^2, \quad (2)$$

where the notation  $f_i(\omega) = f_i(\omega, T, \mu_q)$  is used for the distribution functions, and  $\rho_i$  denotes the spectral function of the partons, while  $d_i$  stand for the degeneracy factors. We note that the derivative of the distribution function accounts for the Pauli-blocking (-) and Bose-enhancement (+) factors. Following Ref. [8], we can evaluate the integral over  $\omega = p_0$  in Eq. (2) by using the residue theorem. When keeping only the leading order contribution in the width  $\gamma(T, \mu_B)$  from the residue - evaluated at the poles of the spectral function  $\omega_i = \pm \tilde{E}(\mathbf{p}) \pm i\gamma$  - we finally obtain:

$$\eta^{\text{RTA}}(T, \mu_q) = \frac{1}{15T} \int \frac{d^3p}{(2\pi)^3} \sum_{i=q,\bar{q},g} \left( \frac{\mathbf{p}^4}{E_i^2 \Gamma_i(\mathbf{p}_i, T, \mu_q)} d_i ((1 \pm f_i(E_i)) f_i(E_i)) \right), \quad (3)$$

which corresponds to the expression derived in the relaxation-time approximation (RTA) [9] by identifying the interaction rate  $\Gamma$  with  $2\gamma$  as expected from transport theory in the quasiparticle limit [10]. We recall that  $\gamma$  is the width parameter in the parton propagator (1). The interaction rate  $\Gamma_i(\mathbf{p}_i, T, \mu_q)$  (inverse relaxation time) is calculated microscopically from the collision integral using the differential cross sections for parton scattering as described in Section

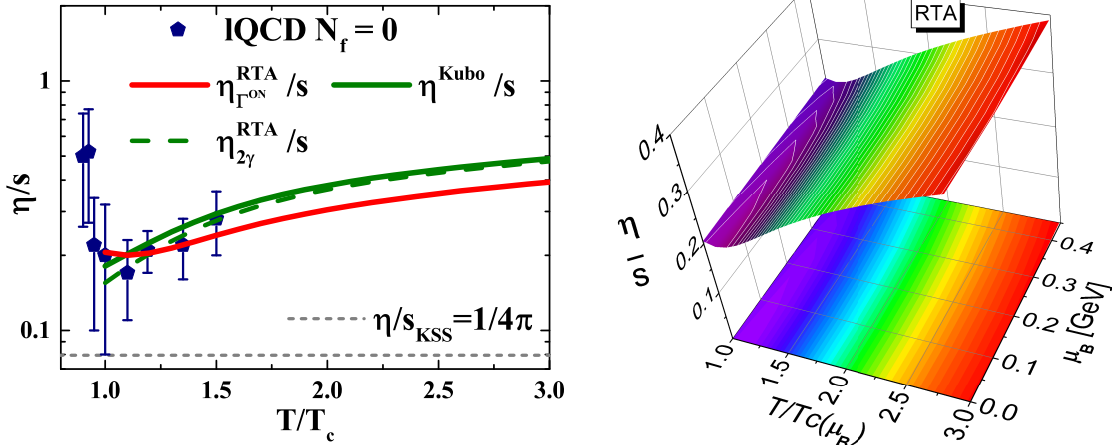


**Figure 1.** (Left) The ratio of shear viscosity to entropy density as a function of the scaled temperature  $T/T_c$  for  $\mu_B = 0$  from Eq. (2-3). The solid green line ( $\eta^{\text{Kubo}}/s$ ) shows the results from the original DQPM in the Kubo formalism while the dashed green line ( $\eta_{2\gamma}^{\text{RTA}}/s$ ) shows the same result in the relaxation-time approximation (3). The solid red line ( $\eta_{\Gamma^{\text{on}}}^{\text{RTA}}/s$ ) results from Eq. (3) using the interaction rate  $\Gamma^{\text{on}}$  calculated by the microscopic differential cross sections in the on-shell limit. The dashed gray line demonstrates the Kovtun-Son-Starinets bound [11] ( $\eta/s$ )<sub>KSS</sub> =  $1/(4\pi)$ . The symbols show IQCD data for pure SU(3) gauge theory taken from Ref. [12] (pentagons). (Right) The ratio of shear viscosity to entropy density as a function of the scaled temperature  $T/T_c$  for  $\mu_B$  in the range  $[0, 0.45]$  GeV from Eq. (3)

2. We, furthermore, recall that the pole energy is  $E_i^2 = p^2 + M_i^2$  where  $M_i$  is the pole mass given in the DQPM.

The actual results are displayed in Fig. 1 for the ratio of shear viscosity to entropy density  $\eta/s$  as a function of the scaled temperature  $T/T_c$  for  $\mu_B = 0$  in comparison to those from lattice QCD [12]. The solid green line ( $\eta^{\text{Kubo}}/s$ ) shows the result from the original DQPM in the Kubo formalism while the dashed green line ( $\eta_{2\gamma}^{\text{RTA}}/s$ ) shows the same result in the relaxation-time approximation (3) by replacing  $\Gamma_i$  by  $2\gamma_i$ . The solid red line ( $\eta_{\Gamma^{\text{on}}}^{\text{RTA}}/s$ ) results from Eq. (3) using the interaction rate  $\Gamma^{\text{on}}$  calculated by the microscopic differential cross sections in the on-shell limit. We find that the ratios  $\eta/s$  do not differ very much and have a similar behavior as a function of temperature. The approximation (3) of the shear viscosity is found to be very close to the one from the Kubo formalism (2) indicating that the quasiparticle limit ( $\gamma \ll M$ ) holds in the DQPM.

We note in passing that there is no strong variation with  $\mu_B$  for fixed  $T/T_c(\mu_B)$ , however, the ratio increases slightly with  $\mu_B$  in the on-shell limit while it slightly drops with  $\mu_B$  in the Kubo formalism for the DQPM [4]. Accordingly, there is some model uncertainty when extracting the shear viscosity in the different approximations.

#### 4. Observables from relativistic nucleus-nucleus collisions

We mention that when implementing the differential cross sections and parton masses into the PHSD5.0 one has to specify the Lagrange parameters  $T$  and  $\mu_B$  in each computational cell in space-time. This has been done by employing the DQPM equation of state, which is practically identical to the lattice QCD equation of state, and a diagonalization of the energy-momentum tensor from PHSD as described in Ref. [4].

Fig. 2 displays the actual results for transverse momentum distributions in case of 10-20% central Au+Au collisions at  $\sqrt{s_{NN}}=19$  GeV for PHSD4.0 (green lines), PHSD5.0 with partonic

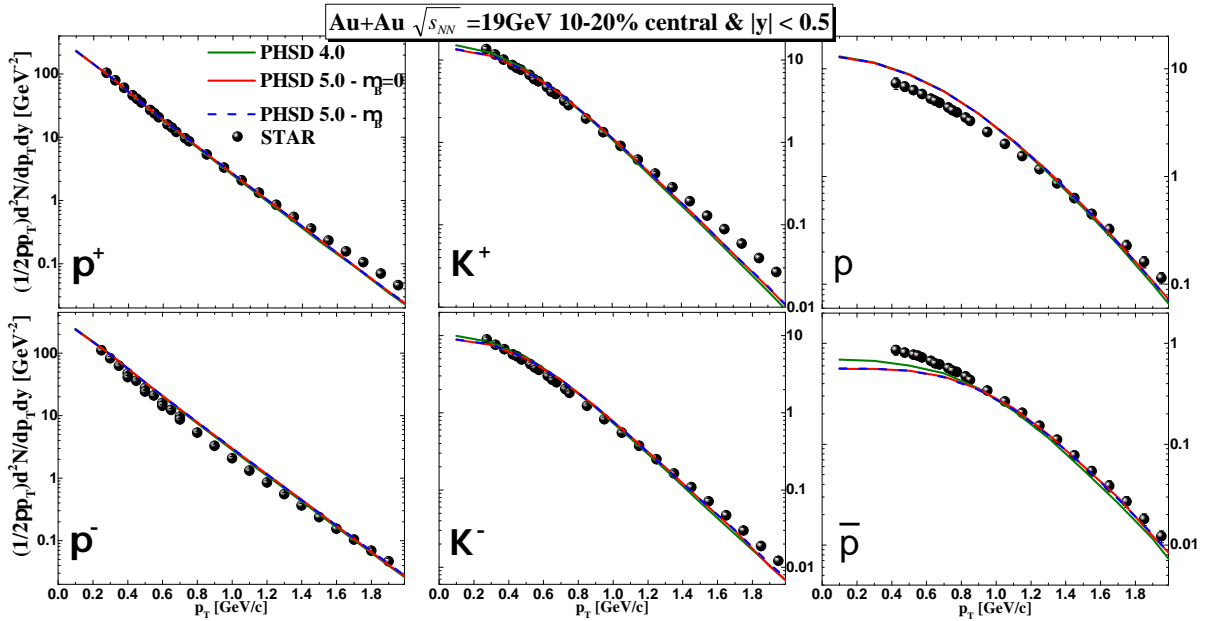


**Figure 2.** The transverse momentum distributions for 10-20% central Au+Au collisions at  $\sqrt{s_{NN}}=19$  GeV and midrapidity ( $|y| < 0.5$ ) for PHSD4.0 (green lines), PHSD5.0 with partonic cross sections and parton masses calculated for  $\mu_B = 0$  (blue dashed lines) and with cross sections and parton masses evaluated at the actual chemical potential  $\mu_B$  in each individual space-time cell (red lines) in comparison to the experimental data from the STAR collaboration [14].

cross sections and parton masses calculated for  $\mu_B = 0$  (blue dashed lines), and with cross sections and parton masses evaluated at the actual chemical potential  $\mu_B$  in each individual space-time cell (red lines) in comparison to the experimental data from the STAR collaboration [14]. Here we focus on the most abundant hadrons, i.e. pions, kaons, protons, antiprotons. We note in passing that the effects of chiral symmetry restoration are incorporated as in Ref. [13] since this was found to be mandatory to achieve a reasonable description of the strangeness degrees of freedom reflected in the kaon and hyperon dynamics. As seen from Fig. 2 there is practically no difference in transverse momentum distributions for all the hadron species from the different versions of PHSD within linewidth which implies that there is no sensitivity to the new partonic differential cross sections and parton masses employed. A comparison to the available experimental data is included (for orientation) but not discussed explicitly since this has been done in more detail in Ref. [13]. This also holds for a variety of hadronic observables from central A+A collisions in the energy range  $5 \text{ GeV} \leq \sqrt{s_{NN}} \leq 200 \text{ GeV}$  which have been considered in Ref. [4].

## 5. Summary and Outlook

We have described the PHSD transport approach and its recent extension to PHSD5.0 [4] to incorporate differential "off-shell cross sections" for all binary partonic channels that are based on the same effective propagators and couplings as employed in the QGP equation of state and the parton propagation. To this end we have calculated the partonic differential cross sections as a function of  $T$  and  $\mu_B$  for the leading tree-level diagrams. These enable us to evaluate partonic scattering rates  $\Gamma_i(T, \mu_B)$  for fixed  $T$  and  $\mu_B$  as well as to compute the ratio of the shear viscosity  $\eta$  to entropy density  $s$  within the Kubo formalism and in RTA in comparison to calculations from lQCD. It turns out that the ratio  $\eta/s$  - calculated with the partonic scattering

rates in the relaxation-time approximation - is very similar to the original result from the DQPM and to lQCD results. Therefore, the present extension of the PHSD approach does not lead to different partonic transport properties in particular at FAIR/NICA energies.

When implementing the differential cross sections and parton masses into the PHSD5.0 approach one has to specify the Lagrange parameters  $T$  and  $\mu_B$  in each computational cell in space-time. This has been done by employing the lattice equation of state and a diagonalization of the energy-momentum tensor from PHSD as described in Ref. [4]. As an example we have shown the results for hadronic transverse momentum spectra from the previous PHSD4.0 [13] with the novel version PHSD5.0 (with and without the explicit dependence of the partonic differential cross sections and parton masses on  $\mu_B$ ) for 10-20% central Au+Au collisions at  $\sqrt{s_{NN}}=19$  GeV. No differences for all hadron "bulk" observables from the various PHSD versions have been found at FAIR/NICA energies within linewidth which implies that there is no sensitivity to the  $\mu_B$ -dependence of the new partonic differential cross sections employed.

Our findings can be understood as follows. The fact that we find only small traces of the  $\mu_B$ -dependence of partonic scattering dynamics in heavy-ion "bulk" observables - although the differential cross sections and parton masses clearly depend on  $\mu_B$  - means that one needs a sizable partonic density and large space-time QGP volume to explore the dynamics in the QGP phase. These conditions are only fulfilled at high bombarding energies (top SPS, RHIC energies) where, however,  $\mu_B$  is rather low. On the other hand, decreasing the bombarding energy to FAIR/NICA energies and, thus, increasing  $\mu_B$ , leads to collisions that are dominated by the hadronic phase where the extraction of information about the parton dynamics will be rather complicated based on "bulk" observables. Further investigations of other observables (such as flow coefficients  $v_n$  of particles and antiparticles, fluctuations and correlations) might contain more distinguishable  $\mu_B$ -traces from the QGP phase.

### Acknowledgments

The authors acknowledge inspiring discussions with J. Aichelin, H. Berrehrach, C. Ratti, E. Seifert, A. Palmese and T. Steinert. This work was supported by the LOEWE center "HIC for FAIR". Furthermore, P.M., L.O. and E.B. acknowledge support by the Deutsche Forschungsgemeinschaft (DFG, German Research Foundation) through the grant CRC-TR 211 'Strong-interaction matter under extreme conditions' - Project number 315477589 - TRR 211. O.S. acknowledges support from HGS-HIRE for FAIR; L.O. and E.B. thank the COST Action THOR, CA15213. The computational resources have been provided by the LOEWE-Center for Scientific Computing.

### References

- [1] Bratkovskaya E L, Cassing W, Konchakovski V P and Linnyk O 2011 *Nucl. Phys. A* **856** 162-182
- [2] Linnyk O, Bratkovskaya E L and Cassing W 2016 *Prog. Part. Nucl. Phys.* **87** 50
- [3] Cassing W and Bratkovskaya E L 2009 *Nucl. Phys. A* **831** 215
- [4] Moreau P, Soloveva O, Oliva L, Song T, Cassing W and Bratkovskaya E 2019 *Phys. Rev. C* **100** 014911
- [5] Kubo R 1957 *J. Phys. Soc. Jpn.* **12** 570
- [6] Ozvenchuk V, Linnyk O, Gorenstein M I, Bratkovskaya E L and Cassing W 2013 *Phys. Rev. C* **87** 064903
- [7] Aarts G and Martinez Resco J M 2002 *J. High Energy Phys.* **04** 053
- [8] Lang R, Kaiser N and Weise W 2012 *Eur. Phys. J. A* **48** 109
- [9] Sasaki C and Redlich K 2009 *Phys. Rev. C* **79** 055207
- [10] Blaizot J.-P. and Iancu E 1999 *Nucl. Phys. B* **557** 183
- [11] Kovtun P K, Son D T and Starinets A O 2005 *Phys. Rev. Lett.* **94** 111601
- [12] Astrakhantsev N, Braguta V and Kotov A 2017 *J. High Energy Phys.* **04** 101
- [13] Palmese A, Cassing W, Seifert E, Steinert T, Moreau P and Bratkovskaya E L 2016 *Phys. Rev. C* **94** 044912
- [14] Adamczyk L et al [STAR Collaboration] 2017 *Phys. Rev. C* **96** 044904